

Utilization of Soft-Switched Boost Converter for MPPT Application in Photovoltaic Single-Phase Grid-Connected Inverter

Ali Haji Ali biglo
*Faculty of Electrical and Computer
 Engineering
 University of Tehran
 Tehran, Iran
 hajjalibiglo@ut.ac.ir*

Saleh Farzamkia
*School of Electrical and Computer
 Engineering
 University of Tehran
 Tehran, Iran
 saleh.farzamkia@yahoo.com*

Shahrokh Farhangi
*Faculty of Electrical and Computer
 Engineering
 University of Tehran
 Tehran, Iran
 farhangi@ut.ac.ir*

Hossein Iman-Eini
*Faculty of Electrical and Computer
 Engineering
 University of Tehran
 Tehran, Iran
 imaneini@ut.ac.ir*

Abstract—This paper presents a modified soft-switched boost converter with a lower number of auxiliary components that provides either zero-voltage-transition (ZVT) or zero-current-transition (ZCT) operation for main switch and diode. Proposed converter is utilized in a single-phase grid-connected photovoltaic power generation system. Due to importance of maximum power harvesting from PV, incremental conductance MPPT algorithm is employed to control DC/DC converter. Several simulation results are provided in PLECS software to validate the effectiveness of proposed soft-switching technique.

Keywords—Soft Switching Boost Converter, Zero-Voltage-Transition (ZVT), Zero-Current-Transition (ZCT), Incremental Conductance MPPT, Single-Phase Grid-Connected Inverter.

I. INTRODUCTION

Energy consumption is growing rapidly, and renewable energies are becoming the best solution because of their several features. Unlike the conventional thermal power plants, renewable energies have no harmful effects on environment. Nowadays, solar energy has a considerable share of generation capacity in several countries such as Germany and China. Since the output voltage of the solar arrays is variable, and its amplitude is lower than the required voltage, a Boost DC-DC converter is usually employed to increase the voltage level and detect the maximum power point (MPP) of PV [1], [2]. Extensive research has been conducted to improve the efficiency, power density, cost and reliability of photovoltaic power generation. Since the hard-switching has a considerable loss, utilizing soft-switching converters could be an effective solution to improve the system's efficiency. Accordingly, the switching frequency of the converter could be increased. The higher switching frequency, the higher power density, and the smaller size of the converter.

Grid-connected photovoltaic system in residential application is a fast-growing technology. In order to increase the efficiency of overall power generation system, many soft-switching PWM converters have been proposed in literature. This feature is achieved by adding some auxiliary components to the main circuit. However, the additional

components increase the cost and complexity of the system as well. For example, reference [3] proposes a soft-switching boost converter where the main switch operates under the zero-voltage condition. In this reference, a resonant circuit is added to the main circuit which consists of one auxiliary switch, two diodes, one resonant inductor, and two capacitors. Reference [4], also, utilizes an auxiliary circuit which is composed of an auxiliary switch, a resonant capacitor, a resonant inductor, and two diodes for providing ZVT for the main switch. Reference [5] proposes a soft-switching boost converter with a lower voltage and current stress on main switch.

However, it has seven additional elements in auxiliary resonant circuit. There are other studies that propose topologies with more switches in the auxiliary circuit [10]. These structures, however, have a lower sufficiency and higher implementation cost. In some PWM soft-switching topologies, the auxiliary switch performs hard switching. Having hard-switching in auxiliary circuit, also, affects the whole system's efficiency. This paper proposes a modified soft-switching boost converter with a low number of auxiliary

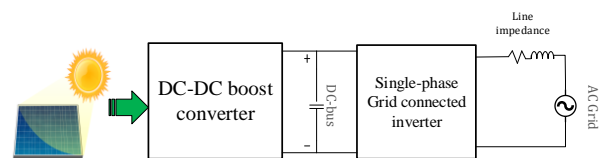


Fig. 1. Diagram of single-phase grid-connected PV power generation

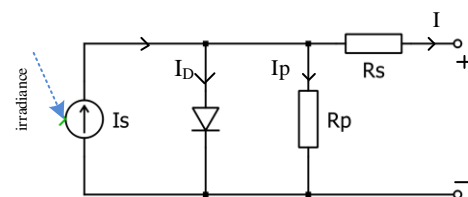


Fig. 2. Equivalent circuit of a PV cells

components. The proposed structure provides either ZVT or ZCT for all main and auxiliary switches and diodes which leads to rise of the converter's efficiency.

The rest of this paper is as follows: In section II, the photovoltaic system is modelled, and characteristics of utilized PV arrays is presented. In section III, the proposed soft-switching boost converter is introduced and different operation modes of this converter is elaborated. In section IV, maximum power point tracking algorithm will be discussed. In this paper, the incremental conductance MPPT technique is applied to DC-DC converter. In section V, simulation results in PLECS environment are provided to validate high performance of the proposed structure. Finally, conclusions are presented in section VI.

II. MODEL AND CHARACTERISTICS OF PHOTOVOLTAIC SYSTEM

Photovoltaic system is a technology that can directly convert the photons' energy to electricity. This process happens in solar cells. In this paper, three parallel-connected KC200GT solar modules with 54 series-connected solar cells are utilized for modelling and simulations. Table I presents more detailed parameters of utilized PV array. Fig. 2 illustrates the equivalent circuit of a PV cell [3]. The equation between voltage and current of solar panel is as follows:

$$I = I_S - I_0 \left\{ e^{\frac{V+IR_S}{nVT}} - 1 \right\} - \frac{V+IR_S}{R_p} \quad (1)$$

where, I is the output current of photovoltaic cells, I_D is reverse saturation current of diode, V is the output voltage, I_P is the parallel current, R_p is the equivalent parallel resistance, R_s is the equivalent series resistance, q is the electron charge ($1.6 \times 10^{-19}C$), K is the Boltzmann constant ($1.38 \times 10^{-23}J / K$), A is the temperature constant, and T is p-n junction temperature ($^{\circ}C$). The output characteristic curves of KC200GT solar modules in different irradiances and different temperatures are shown in Fig. 3. As it can be seen, the output power of the PV cell increases when the irradiance is increased and decreases when the temperature is increased.

III. PROPOSED SOFT-SWITCHED BOOST CONVERTER

Soft-switching techniques are divided into two categories; variable frequency and fixed frequency (or PWM) soft-switching. Variable frequency soft-switching techniques have a more complicated control system. Indeed, optimized design of magnetic elements is quite complex. In PWM soft-switching techniques, active elements of converter can operate in zero-voltage-transition (ZVT), zero-current-transition (ZCT), or combination of both mentioned conditions. These converters have auxiliary circuits which consist of power, inductor, capacitor, and base for the transducer of the switches [4], [5].

Fig. 5 illustrates the proposed soft-switched boost converter. The auxiliary circuit in this structure consists of one resonant capacitor (C_r), one resonant inductor (L_r), one auxiliary switch (S_2) and one auxiliary diode (D_2). Since L_s is large enough, the combination of input voltage source and L_s could be considered as a constant current source (I_s). The switch S_1 turns on at ZVZCT condition and turns off at approximately ZVT condition. As ZVZCT can be seen in Fig. 5, six operation stages exist in each cycle. Fig. 6 shows the various waveforms of the proposed converter which are obtained from simulation in PLECS software. Different operating modes of converter are as follows:

TABLE I: parameter values of PV array used in simulation

Indicator	Parameter	Value
N	Series connected PV	3
N_S	number of solar cells in a string in solar array	54
N_P	number of solar cell strings in parallel solar array	3
T_N	nominal temperature of solar cells	25 ($^{\circ}C$)
G_N	nominal irradiation of solar cells	1000 ($\frac{W}{m^2}$)
V_{OC}	open circuit voltage of array	32.9 (V)
I_{SC}	short circuit current of array	8.21 (A)
R_P	equivalent series resistance of array	0.221 (Ω)

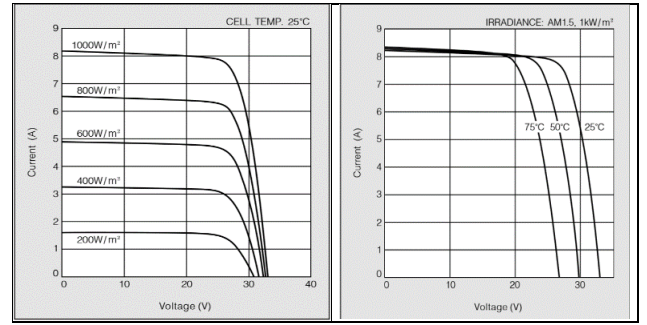


Fig. 3. The output characteristics curves of KC200GT solar module

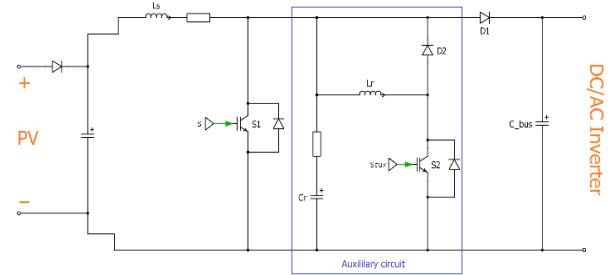


Fig. 4. Proposed soft-switching boost converter

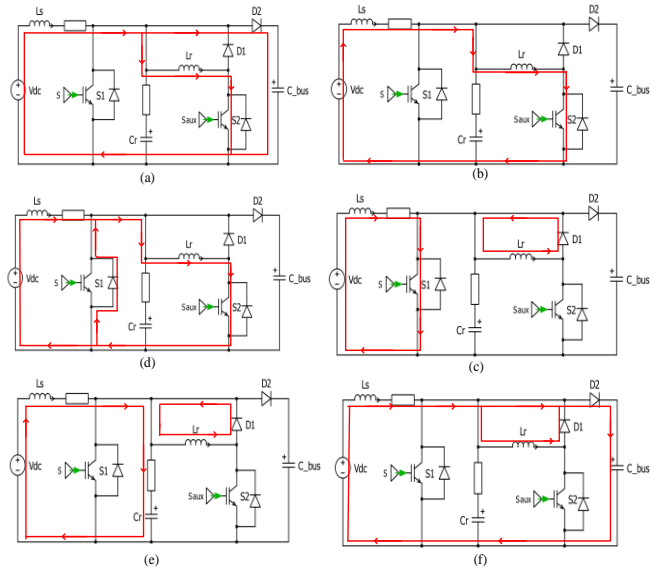


Fig. 5. Operational modes of the soft-switching boost converter for the PV generation system waveforms according to operational intervals.

TABLE II: parameter values of circuit used in simulation

Parameter	Indicator	Value
Maximum power	$P_{O\max}$	1600 [w]
Switching frequency	f_{sw}	20 [KHz]
PV modules output	V_S	50-100 [v]
DC-bus voltage	V_{bus}	400 [V]
Main inductor	L_S	1 [mH]
DC-bus capacitor	C_{bus}	1000 [μ F]
Resonant inductor	R_r	4.4 [μ H]
Resonant capacitor	C_r	800 [pF]
Main switch	S1	IKW30N60H3
Main diode	D2	RHRG75120
Auxiliary switch	S2	KA10N60T
Grid-side voltage	V_{grid}	230 RMS [V]
Grid frequency	f_{grid}	50 [Hz]
Line resistance	R_L	0.15 [Ω]
Line inductor	L_L	5 [mH]

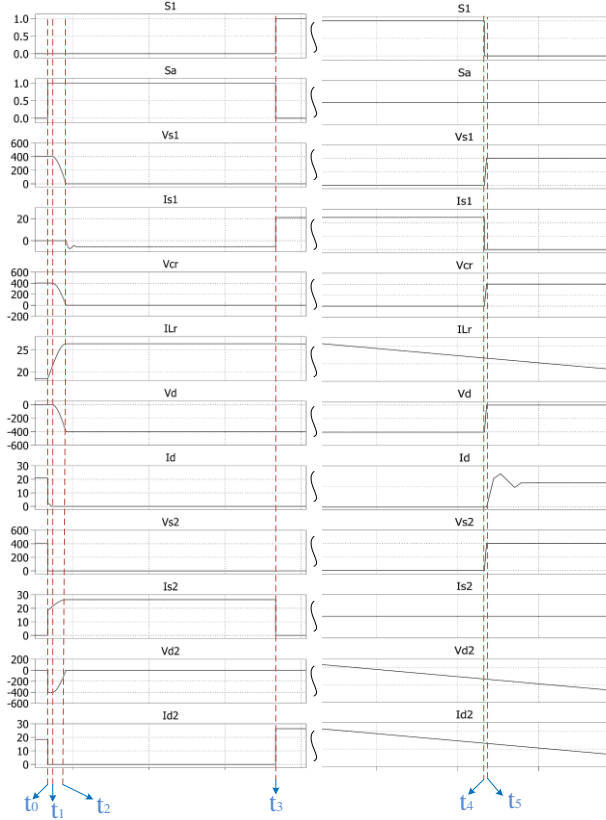


Fig. 6. Waveforms of soft-switching boost converter.

- Mode ($t_0 \leq t < t_1$): At the beginning, both of main and auxiliary switches are OFF. Diode D1 is conducting the current I_S . At t_0 , the auxiliary diode turns on. The current of L_r increases linearly until it reaches to I_S at t_1 . Simultaneously, the current of D1 decreases linearly until it reaches to zero at t_1 .
- Mode ($t_1 \leq t < t_2$): At t_1 , the inductor L_r starts to resonate with C_r . Consequently, the I_{Lr} increases and discharges the C_r . This mode ends when the voltage of C_r becomes zero.
- Mode ($t_2 \leq t < t_3$): In this mode, voltage across S1 is zero. I_{Lr} passes through body diode of S1. This current guarantees the ZVT activation of S1.

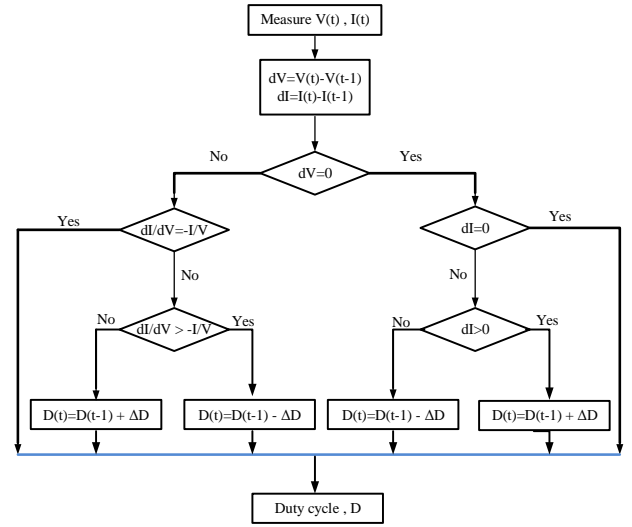


Fig. 7. Flowchart of Incremental Conductance algorithm

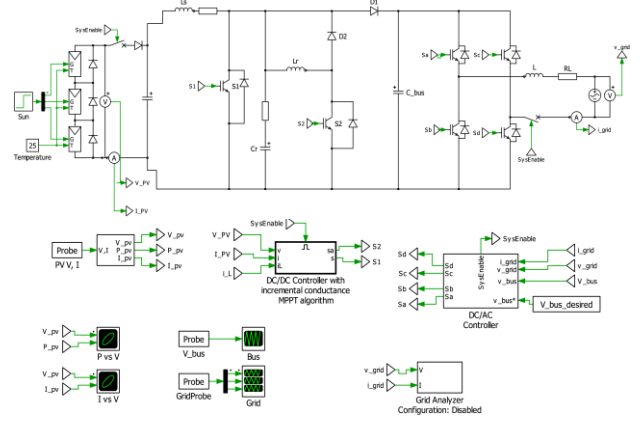


Fig. 8. Simulation diagram in PLECS software.

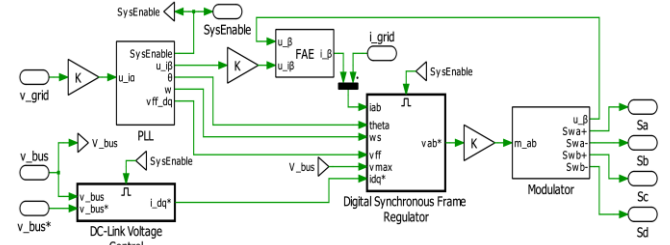


Fig. 9. Control system of DC/AC grid-connected inverter.

- Mode ($t_3 \leq t < t_4$): At t_3 , S1 turns on at ZVT condition. Synchronously, S2 turns off. This operation mode is as similar to the conventional boost converter.
- Mode ($t_4 \leq t < t_5$): the S1 is turned off at t_4 , and C_r starts to charge until V_{Cr} reaches to output voltage at t_5 . The C_r helps the voltage of S1 to increase slowly. Therefore, the switching losses is reduced during turn off process.
- Mode ($t_5 \leq t < t_0$): Finally, when voltage across D1 attained to zero, D1 starts conducting I_S . Consequently, the energy stored in the resonant inductor is transferred to the load during this time interval.

IV. MAXIMUM POWER POINT TRACKING

Tracking the maximum power point (MPP) of a photovoltaic (PV) array is an essential part of a PV system.

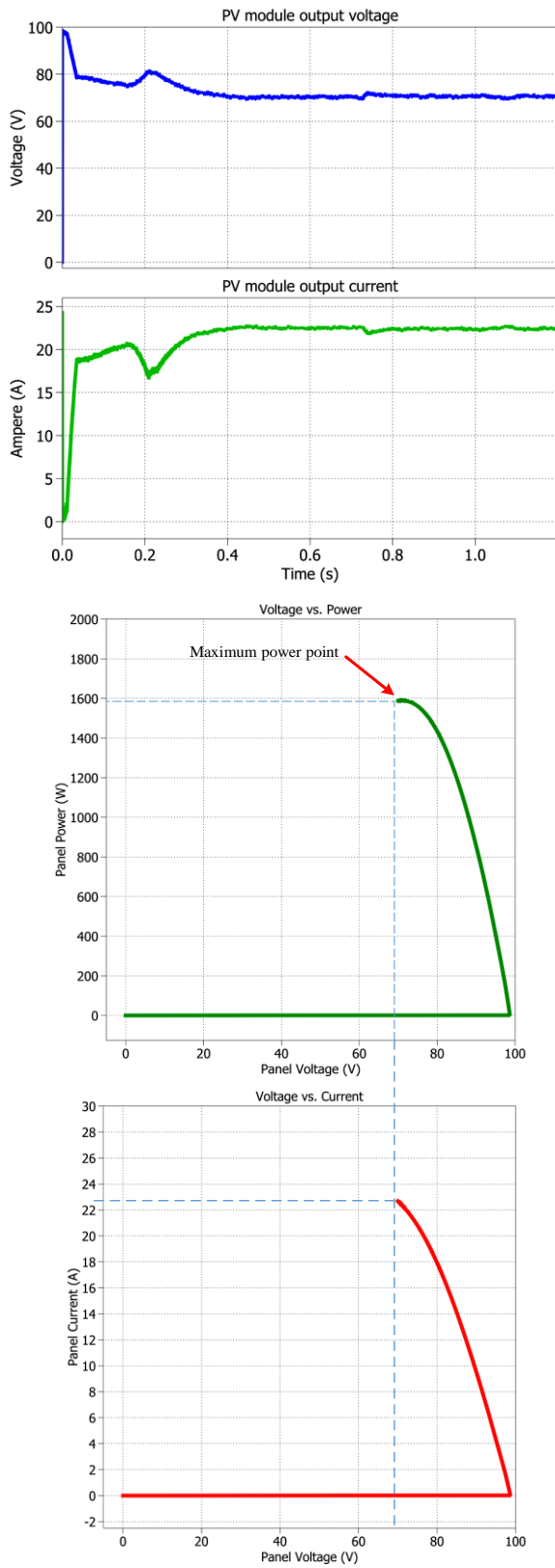


Fig. 10. Simulation results of output characteristic curves of PV module. (a) Simulated real-time waveforms of voltage, and current. Simulated I-V and power curves of PV module. (b) Simulated V-P and V-I curves of PV module.

Many algorithms and techniques of MPPT have been introduced which can reach maximum power under different radiation conditions and temperatures. However, most of

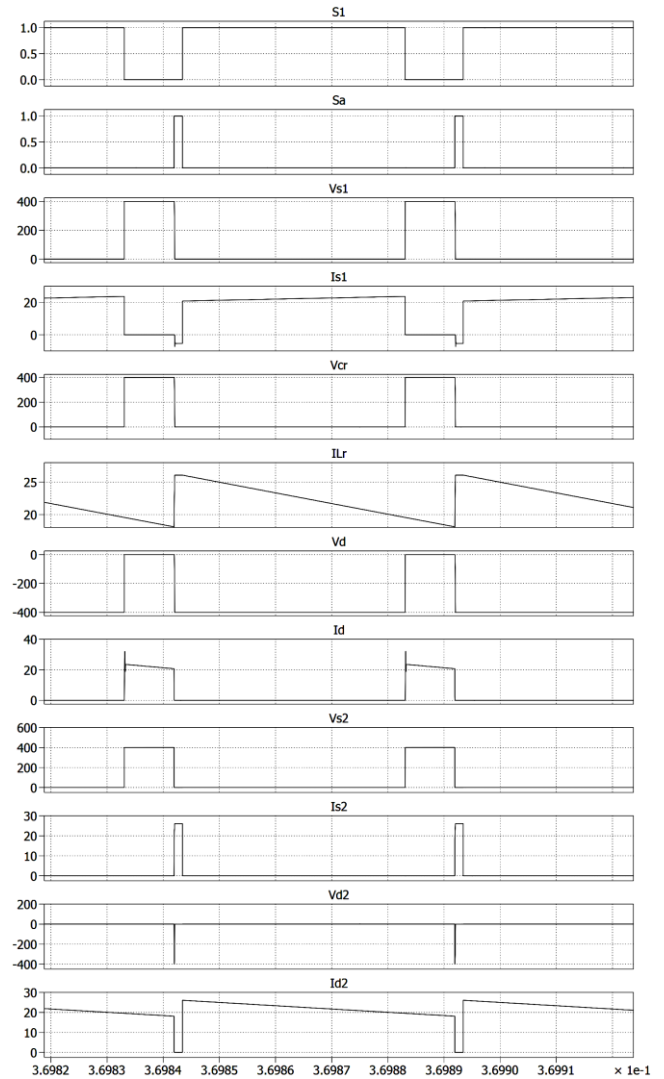
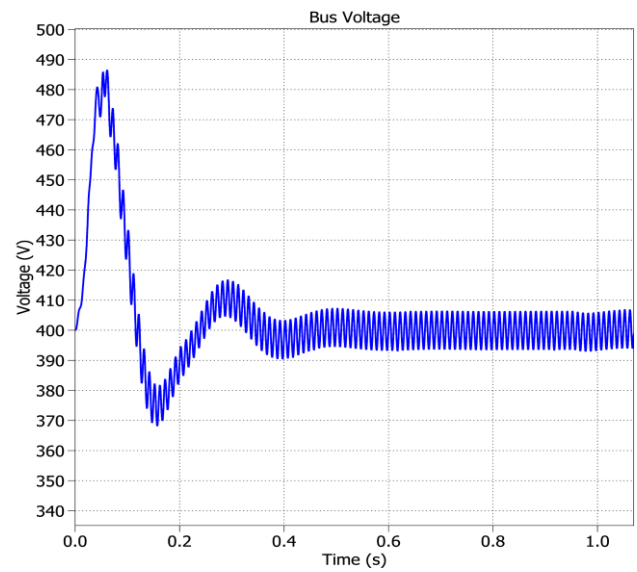


Fig. 11. Voltage and current of soft-switched boost converter's elements.



(a)

these techniques are not commercial. Perturb and observe (P&O) and incremental conductance (IC) are the most commonly used techniques for MPPT [6]. The P&O algorithm is simple and easy. This method, however, has slow response with rapidly changing operation condition. Incremental conductance has a fast response to rapidly changing atmospheric conditions and stable output [1]. The incremental conductance techniques are based on the fact that the slope of the PV array power curve is zero at the MPP, negative on the right hand of MPP, and positive on the left of the MPP. The theoretical analysis of this method is explained as follows.

$$\frac{dP}{dV} = 0 \quad \text{at MPP} \quad (2)$$

$$\frac{dP}{dV} > 0 \quad \text{at left of MPP} \quad (3)$$

$$\frac{dP}{dV} < 0 \quad \text{at right of MPP} \quad (4)$$

$$P = V \cdot I \quad (5)$$

$$\frac{dP}{dV} = \frac{d(VI)}{dV} = I \frac{dV}{dV} + V \frac{dI}{dV} = I + V \frac{dI}{dV} \quad (6)$$

Therefore, equations (1) to (3) can be rewritten as follows:

$$\frac{dI}{dV} = -\frac{I}{V} \quad \text{at MPP} \quad (7)$$

$$\frac{dI}{dV} > -\frac{I}{V} \quad \text{at left of MPP} \quad (8)$$

$$\frac{dI}{dV} < -\frac{I}{V} \quad \text{at right of MPP} \quad (9)$$

Hence, the MPP can be tracked by comparing the instantaneous conductance (I/V) to the incremental conductance ($\Delta I/\Delta V$). Flowchart of incremental conductance is shown in Fig. 7.

V. SIMULATION RESULTS

The single-phase grid-connected photovoltaic power generation system with PV module and soft-switched boost converter is simulated using PLECS software. The simulation results demonstrate the operation of a grid-tied solar inverter at its MPP. Fig. 8 shows the circuit model in the PLECS environment. The detailed parameters of the simulated system are presented in Table II.

The output of the boost converter is connected to the DC-side of a single-phase voltage source inverter (VSI) via a DC-link capacitor. The VSI is regulated by a nested control scheme with an outer voltage loop and an inner current loop [7]. The outer voltage loop is used to control the DC-link voltage and maintain the voltage at the desired level. The voltage loop generates the set point of the grid current amplitude. Since the converter is operated with zero reactive power, the generated current set point from the voltage controller is equal to the set point of the q-axis current in the synchronous frame regulator. Fig. 9 shows the control system of DC/AC grid-connected inverter [8], [9]. Fig. 10(a) shows

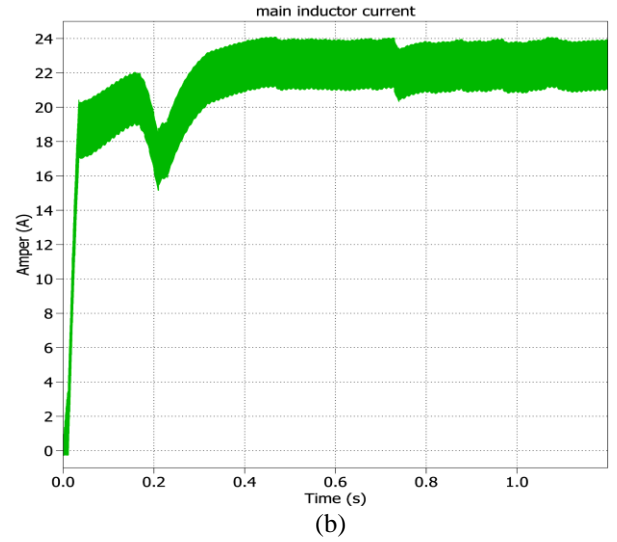


Fig. 12. (a) voltage of DC_bus capacitor (V_{Cr}). (b) and current of main inductor (I_{Ls})

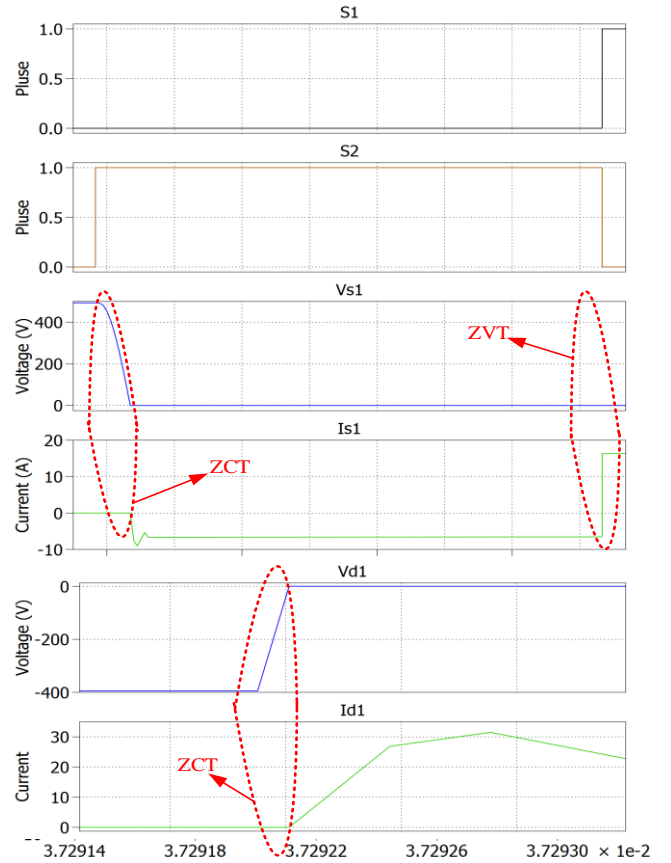


Fig. 13. closer view of diode and switch ZVT, ZCT operation.

the PV modules output voltage and current in time domain. Fig. 10(b), also, depicts the V-I and V-P curves for the maximum power point. Based on these curves, the output voltage and current of PV modules at MPP are 70.1 V and 22.7 A. In Fig. 11, also, two period of soft-switched boost converter parameters are provided. In Fig. 12, voltage of DC bus capacitor (V_{Cr}) and current of main inductor (I_{Ls}) are shown. These waveforms verify that VDC-bus is stabilized on 400 V and ripple of ILr is appropriate. Moreover, Fig. 13

gives a closer view of diode and switch ZVT, ZCT operation. Fig.14 shows the grid-side voltage, current and power. The grid-side voltage is measured at the output of the DC/AC inverter. Fig. 15, also, shows the efficiency comparison between hard switching and soft switching boost converter. It is worth to mentioning that only power losses of IGBTs and diodes are taken into account. The power loss in passive component such as inductors and capacitors are neglected. Efficiency of boost converter estimated in simulation under total range of load, from 100% load to 10% nominal output power.

VI. CONCLUSION

This paper introduces a modified soft-switching boost converter with minimum auxiliary component that can operate at either ZVT or ZCT for main switch and Diode. Soft-switched boost converter is controlled by incremental conductance MPPT algorithm. This converter has simple control scheme same as traditional boost converter. The design of a soft-switched boost converter is similar to the conventional boost converter because the duration interval of auxiliary circuit is much shorter than duty cycle of main switch and main diode. The proposed converter can be utilized to a stand-alone or a grid-connected system using a PV power conditioning system. Simulation results verify the applicability of proposed topology and demonstrate outcome of this research. All simulations are done in PLECS software environment.

REFERENCES

- [1] Q. Li and P. Wolfs, "A review of the single phase photovoltaic module integrated converter topologies with three different DC link configurations," *IEEE Trans. Power Electron.*, vol. 23, no. 3, pp. 1320–1333, 2008.
- [2] S. Rezayi, H. Iman-Eini, M. Hamzeh, S. Bacha, and S. Farzamkia, "Dual-output DC/DC boost converter for bipolar DC microgrids," *IET Renew. Power Gener.*, vol. 13, no. 8, pp. 1402–1410, 2019.
- [3] S.-H. Park, S.-R. Park, J.-S. Yu, Y.-C. Jung, and C.-Y. Won, "Analysis and design of a soft-switching boost converter with an HI-bridge auxiliary resonant circuit," *IEEE Trans. Power Electron.*, vol. 25, no. 8, pp. 2142–2149, 2010.
- [4] G.-H. Cho, "A new zero voltage switching resonant DC-link inverter with low voltage stress," 1991.
- [5] E. S. da Silva, L. dos Reis Barbosa, J. B. Vieira, L. C. de Freitas, and V. J. Farias, "An improved boost PWM soft-single-switched converter with low voltage and current stresses," *IEEE Trans. Ind. Electron.*, vol. 48, no. 6, pp. 1174–1179, 2001.
- [6] O. Waszynczuk, "Dynamic behavior of a class of photovoltaic power systems," *IEEE Trans. power Appar. Syst.*, no. 9, pp. 3031–3037, 1983.
- [7] S. Jain and V. Agarwal, "A single-stage grid connected inverter topology for solar PV systems with maximum power point tracking," 2007.
- [8] Y. Liu, B. Ge, H. Abu-Rub, and F. Z. Peng, "Phase-shifted pulse-width-amplitude modulation for quasi-Z-source cascade multilevel inverter-based photovoltaic power system," *IET Power Electron.*, vol. 7, no. 6, pp. 1444–1456, 2014.
- [9] F. Z. Peng, M. Shen, and K. Holland, "Application of Z-source inverter for traction drive of fuel cell—Battery hybrid electric vehicles," *IEEE Trans. Power Electron.*, vol. 22, no. 3, pp. 1054–1061, 2007.

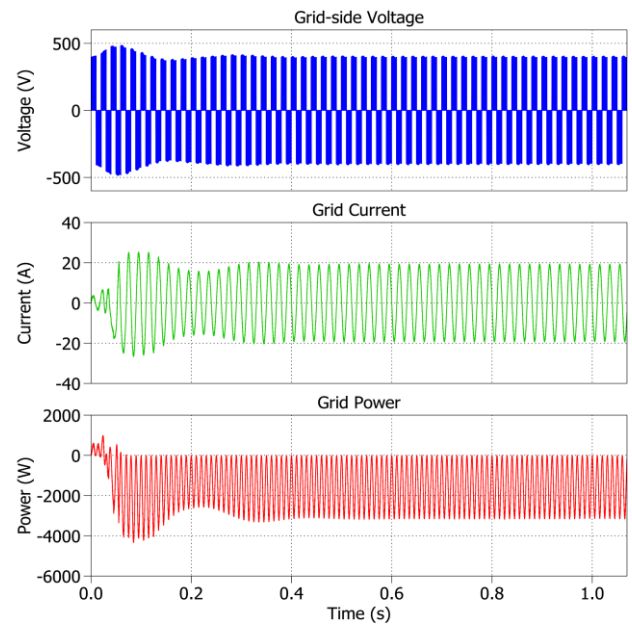


Fig.14. grid-side voltage, current and power

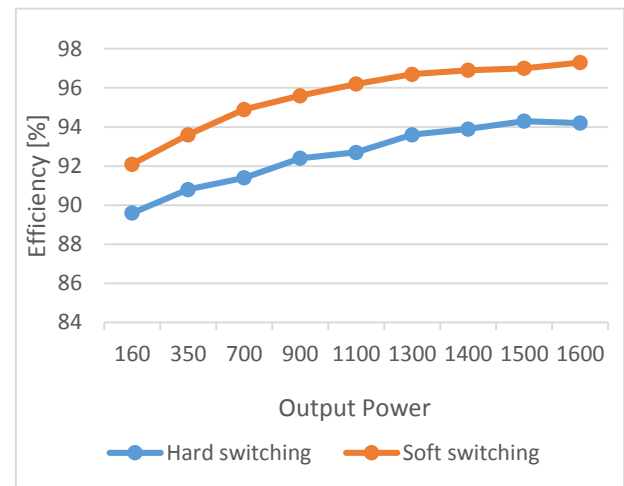


Fig.15. Efficiency of boost converter

- [10] Dong-Woo Han, Hee-Jun Lee, Soo-Cheol Shin, Jun-Gu Kim, Y. Jung and C. Won, "A new soft switching ZVT boost converter using auxiliary resonant circuit," *2012 IEEE Vehicle Power and Propulsion Conference*, Seoul, 2012, pp. 1250-1255